



Polymer complexes. LXXI. Spectroscopic studies, thermal properties, DNA binding and antimicrobial activity of polymer complexes

M.A. Diab¹ | A.Z. El-Sonbati¹ | Sh.M. Morgan² | M.A. El-Mogazy¹

¹ Chemistry Department, Faculty of Science, Damietta University, Damietta, Egypt

² Environmental Monitoring Laboratory, Ministry of Health, Port Said, Egypt

Correspondence

Sh.M. Morgan, Environmental Monitoring Laboratory, Ministry of Health, Port Said, Egypt.

Email: shimaa_mohamad2010@yahoo.com

Polymer complexes of Co(II), Ni(II), Mn(II), Cr(III) and Cd(II) were prepared by the reaction of 3-allyl-5-[(4-nitrophenylazo)]-2-thioxothiazolidine-4-one (HL) with metal ions. The structure of polymer complexes was characterized by elemental analysis, IR, UV-Vis spectra, X-ray diffraction analysis, magnetic susceptibility, conductivity measurements and thermal analysis. Reaction of HL with Co(II), Ni(II), Mn(II), Cr(III) and Cd(II) ions (acetate or chloride) give polymer complexes (**1–5**) with general stoichiometric $[M(L)(O_2CCH_3)(H_2O)_2]_n$ (where L = anionic of HL and M = Co(II) (**1**) or Ni(II) (**2**)), $[Mn(HL)_2(OCOCH_3)_2]_n$ (**3**), $[Cr(L)_2(Cl)(H_2O)]_n$ (**4**) and $[Cd(HL)(O_2CCH_3)_2]_n$ (**5**). The value of HOMO-LUMO energy gap (ΔE) for forms (A-C) of monomer (HL) is 2.529, 2.296 and 2.235 eV, respectively. According to ΔE value, compound has minimum ΔE is the more stable, so keto hydrazone form (C) is more stable than the other forms (azo keto form (A), azo enol form (B)). The interaction between HL, polymer complexes of Co(II), Ni(II), Mn(II), Cr(III) and Cd(II) with Calf thymus DNA showed hypochromism effect. The HL and its polymer complexes were tested against some bacterial and fungal species. The results showed that the Cr(III) polymer complex (**4**) has more antibacterial activity than HL and polymer complexes (**1–3** and **5**) against *Bacillus subtilis*, *Staphylococcus aureus* and *Salmonella typhimurium*.

KEYWORDS

antimicrobial activity, DNA binding study, polymer complexes, quantum chemical parameters, thermal analysis

1 | INTRODUCTION

Azo compounds are known for widespread applications in various fields and have been attention of synthetic and theoretical chemists. They are the subject of large research works due to their applications as textile dye,^[1] pharmaceuticals^[2,3] and indicators.^[4] Azo dyes derived from heterocyclic amine or derivatives aniline containing nitrogen in their aromatic rings and their metal complexes have been receiving the attention of research

groups due to their biological activities as antitumor,^[5] antibacterial^[6] and antifungal.^[7] These compounds are now in good demands as optical and conducting organic materials.^[8–11] Azo dyes derived from derivatives aniline moiety and its metal complexes have variety of applications in biological, analytical and pharmacological areas.

A literature survey shows subtle work to synthesis and characterization of rhodanine azo dyes, also their metal complexes which widely used in different fields

such as biological studies, optical and electrical studies.^[8,9,12] Transition metal polymer complexes of allyl rhodanine azo compounds are a subject of current and growing interest and that may have numerous applications chemically allyl azo rhodanine containing oxygen, sulphur and nitrogen donor atoms are of great interest because of their great versatility as ligands,^[6,13] due to presence of several potential donor atoms, their ability and flexibility to coordinate in either deprotonated or neutral form.

The reaction of metal ions with polymeric ligands containing pendant functional groups, which act as chelating groups in binding polyvalent metal ions, produces coordinated systems which possibly have enhanced thermal stability and thereby improved chemical resistance.^[14]

The present work describes the chelation behavior of 3-allyl-5-[(4-nitrophenylazo)]-2-thioxothiazolidine-4-one (HL) monomer towards to Co(II), Ni(II), Mn(II), Cr(III) and Cd(II) ions (acetate or chloride). The structure of the M(II) and Cr(III) polymer complexes is characterized by elemental analysis, IR, UV-Vis spectra and thermal analysis. The optimized geometry and quantum chemical parameters such as highest occupied molecular orbital energy, the lowest unoccupied molecular orbital energy and HOMO-LUMO energy gap for HL are discussed. The antimicrobial activity of HL and its polymer complexes were discussed. The thermodynamic parameters are calculated using Coats-Redfern and Horowitz-Metzger methods.

2 | EXPERIMENTAL

2.1 | Material and reagents

3-Allyl-2-thioxothiazolidin-4-one and 4-nitroaniline were bought from Aldrich. 2,2'-Azobisisobutyronitrile (AIBN) was purified by dissolving in hot ethanol and filtering. $M(\text{CH}_3\text{COO})_2 \cdot 4\text{H}_2\text{O}$ ($M = \text{Co(II)}, \text{Ni(II)}$ and Mn(II)),

$\text{Cd}(\text{CH}_3\text{COO})_2 \cdot 2\text{H}_2\text{O}$ and $\text{CrCl}_3 \cdot 6\text{H}_2\text{O}$ from Sigma Aldrich. Organic solvents (diethyl ether, dimethylformamide (DMF), dimethylsulfoxide (DMSO) and ethanol) were bought from BDH. The calf thymus DNA (CT-DNA) was acquired from SRL (India).

2.2 | Preparation of 3-allyl-5-[(4-nitrophenylazo)]-2-thioxothiazolidine-4-one (HL) monomer

3-Allyl-5-[(4-nitrophenylazo)]-2-thioxothiazolidine-4-one (HL) monomer was synthesized by the well-established standard method (Figure 1).^[6,13] The resulting solid of HL was recrystallized with ethanol and then dried in a vacuum desiccator over anhydrous calcium chloride. Analytical found for HL monomer ($\text{C}_{12}\text{H}_{10}\text{N}_4\text{O}_3\text{S}_2$): C, 44.60; H, 3.00; N, 17.66; S, 20.12% and calculated: C, 44.72; H, 3.11; N, 17.39; S, 19.88%.

IR (KBr, ν_{max} , cm^{-1}): 3391–3255 (N–H str.), 3079 (=C–H str.), 3013 (C–H str. asym.), 2927 (C–H str. sym.), 1557 (C=C, phenyl ring), 1495 (δNH), 1702 [$\nu(\text{C}=\text{O})$], 1604 (–C=N– hydrazone), 1138 (–N–N–), 842 (C=S), 795 (N–H wag).

^1H NMR: (DMSO- d_6), δ (ppm): 7.48–8.25 (d, Ar, 4H), 11.64 (NH, hydrazone, exchangeable with D_2O), 5.80 (s, $\text{CH}_2 = \text{CH}$) for the vinyl CH proton and δ (4.60 (*cis*), 5.25 (*trans*)) for the vinyl CH_2 protons, these peaks disappeared on polymerization.

The mass spectrum of HL shows that the mass of 322 amu related to formula ($\text{C}_{12}\text{H}_{10}\text{N}_4\text{O}_3\text{S}_2$) as shown in Figure S1. It is obvious that, the molecular ion peaks are in good agreement with their suggested empirical formula as indicated from elemental analysis (Table 1). The ion of $m/z = 322$ amu fragmented to stable peak at $m/z = 306$ by loss oxygen atom as shown in Scheme 1 (structure I). The peaks corresponding to various fragments in HL appeared at $m/z = 195$ amu (structure II), 149 amu (structure III) and 63 amu (structure IV) by loss $\text{C}_5\text{H}_5\text{NS}$, NO_2 and $\text{C}_2\text{H}_2\text{N}_2\text{S}$ atoms, respectively.

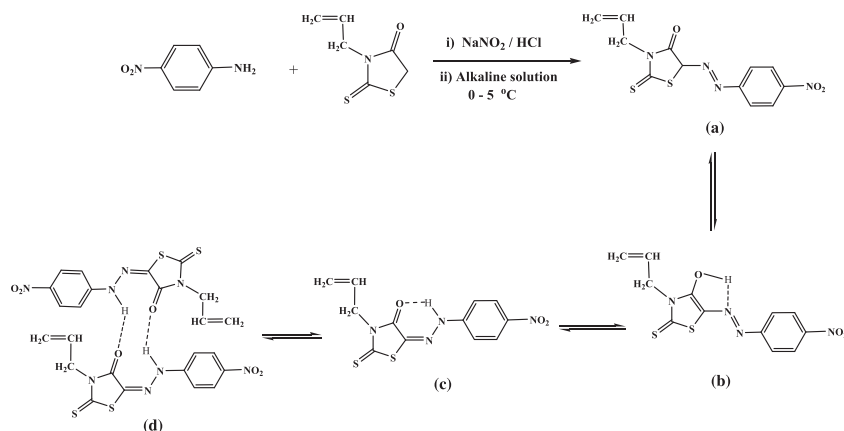
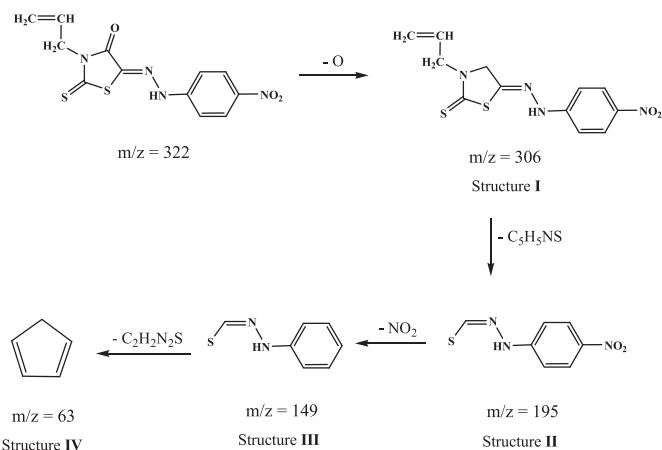


FIGURE 1 Tautomeric structures of the monomer

TABLE 1 Elemental analysis of HL and its polymer complexes (1–5)

Compound	Exp. (calcd.)%				
	C	H	N	S	M
HL	44.60 (44.72)	3.00 (3.11)	17.66 (17.39)	20.12 (19.88)	-
[Co(L)(O ₂ CCH ₃)(H ₂ O) ₂] _n (1)	35.22 (35.37)	3.26 (3.37)	11.58 (11.79)	13.36 (13.48)	12.44 (12.41)
[Ni(L)(O ₂ CCH ₃)(H ₂ O) ₂] _n (2)	34.96 (35.39)	3.21 (3.37)	11.69 (11.80)	13.34 (13.48)	12.30 (12.36)
[Mn(HL) ₂ (OCOCH ₃) ₂] _n (3)	40.94 (41.13)	3.21 (3.18)	13.59 (13.71)	15.45 (15.67)	6.66 (6.73)
[Cr(L) ₂ (Cl)(H ₂ O) _n (4)	38.49 (38.53)	2.55 (2.68)	14.82 (14.98)	17.03 (17.12)	7.31 (6.96)
[Cd(HL)(O ₂ CCH ₃) ₂] _n (5)	34.39 (34.76)	2.78 (2.90)	10.04 (10.14)	11.42 (11.59)	20.49 (20.35)

**SCHEME 1** The fragmentation patterns of mass spectrum of HL

2.3 | Preparation of the polymer complexes

Polymer complexes were prepared by refluxing M(II) (M = Co(II), Ni(II), Mn(II) and Cd(II) acetate) and Cr(III) chloride (0.001 mol) with the HL (0.001 mol) in 20 ml DMF as a solvent, and 0.1% (w/v) AIBN as initiator and the resulting mixture was heated at reflux for ~ 8 hours. The hot solution was precipitated by pouring in large excesses of distilled water containing dilute hydrochloric acid, to remove the metal ions that were incorporated into the polymer complexes. The polymer complexes (1–5, see Table 1) were filtered, washed with water, and dried in a vacuum oven at 40 °C for several days. All the polymer complexes are soluble in dimethylformamide (DMF) and dimethylsulfoxide (DMSO).

2.4 | Study the DNA binding

The DNA binding study of the monomer and polymer complexes to Calf thymus DNA (CT-DNA) was studied by absorption spectra.^[15,16] Electronic absorption spectra are carried out using 1 cm quartz cuvette at room temperature by fixing the concentration of monomer or polymer complexes (1×10^{-3} mol L⁻¹), while progressively

increasing the concentration of calf thymus DNA (CT-DNA). The intrinsic binding constant (K_b) of the monomer and polymer complexes with calf thymus DNA was determined.^[15,16] The intrinsic binding constant (K_b) of the HL and its polymer complexes is determined by the following equation:^[15]

$$\frac{[DNA]}{(\epsilon_a - \epsilon_f)} = \frac{[DNA]}{(\epsilon_b - \epsilon_f)} + \frac{1}{K_b(\epsilon_a - \epsilon_f)} \quad (1)$$

where ϵ_a is the molar extinction coefficient observed for the $A_{obs}/[\text{monomer or polymer complex}]$ at the specific DNA concentration, ϵ_f is the molar extinction coefficient of the free monomer or polymer complex in solution, $[DNA]$ is the concentration of CT-DNA in base pairs and ϵ_b is the molar extinction coefficient of the monomer (HL) or polymer complex when fully bound to DNA.

2.5 | Methodology of antimicrobial activity

The monomer (HL) and its polymer complexes (1–5) of 10 mg/ml concentration were tested for their antibacterial and antifungal activities. The tested compounds were evaluated against two Gram positive bacteria (*Bacillus*

subtilis and *Staphylococcus aureus*), two Gram negative bacteria (*Escherichia coli* and *Salmonella typhimurium*) and two fungal species (*Aspergillus fumigatus* and *Candida albicans*) by diffusion agar technique.^[17] Well diameter (6 mm) was made in the media and the hole was loaded with the compounds. All compounds were placed at four equidistant places at a distance of 2 cm from the center in the inoculated Petriplates. Dimethylsulfoxide (DMSO) was served as control. Finally, all Petri dishes were incubated at 37 °C and 30 °C after 48 hour and 7 days for bacteria and fungi, respectively, where inhibition zones were detected around each disk. Ketoconazole was taken as a reference for the antifungal effect and Gentamycin was used as standard for the evaluation of antibacterial activity. All experiments were performed in triplicate, and data plotted were the mean value.

2.6 | Analytical measurements

Elemental microanalysis of the separated compounds for C, H, N and S were analyzed in the Microanalytical Center, Cairo University, Egypt. Metal ions were determined by standard methods.^[18] The ¹H NMR spectra were obtained with a JEOL FX90 Fourier transform spectrometer with DMSO-d₆ as the solvent and using tetramethylsilane (TMS) as an internal standard. The molar conductance was carried out by Sergeant Welch Scientific Co., Skokie, IL, USA. The magnetic moment of the prepared solid complexes was determined at room temperature using the Gouy's method. Mercury(II) (tetrathiocyanato)cobalt(II), [Hg{Co(SCN)₄}], was used for the calibration of the Gouy tubes. Magnetic moments were calculated using the equation, $\mu_{\text{eff.}} = 2.84[\text{Tc}_M^{\text{coord.}}]^{1/2}$. Diamagnetic corrections were calculated from the values given by Selwood^[19] and Pascal's constants. Mass spectrum was recorded by the EI technique at 70 eV using MS-5988 GS-MS Hewlett-Packard. Infrared spectra were recorded as KBr discs using a Perkin-Elmer 1340 spectrophotometer. Ultraviolet-visible spectra of the compounds were recorded in nujol mulls using a Unicomp SP 8800 spectrophotometer. Thermal studies were computed on Simultaneous Thermal Analyzer (STA) 6000 system using thermogravimetric analysis (TGA) method. Thermal properties of the samples were analyzed in the temperature range from 30 to 800 °C at the heating rate of 10 °C/min under dynamic nitrogen atmosphere. X-ray diffraction analysis of compounds was recorded on X-ray diffractometer analysis in the range of diffraction angle $2\theta^\circ = 4\text{--}80^\circ$.^[15] This analysis was carried out using CuK α radiation. The applied voltage and the tube current are 40 kV and 30 mA, respectively.

The molecular structures of the compounds were optimized by HF method with 3-21G basis set. The molecules were built with the Perkin Elmer ChemBio Draw and optimized using Perkin Elmer ChemBio3D software.^[15,16]

Docking calculations were carried out on receptors of the androgen receptor prostate cancer mutant H874Y ligand binding domain bound with testosterone and a TIF2 box3 coactivator peptide 740–753 (PDB code: 2Q7L Hormone) and crystal structure of the BRCT repeat region from the breast cancer associated protein, BRCA1 (1JNX Gene regulation).^[20–22]

3 | RESULTS AND DISCUSSION

3.1 | Geometrical structure and molecular docking of HL

Geometrical structure of the keto hydrazone form (C) of HL is shown in Figure 2. The highest occupied molecular orbital (HOMO) and lowest unoccupied molecular orbital (LUMO) for keto hydrazone form (C) of HL is presented in Figure S2. Quantum chemical parameters of forms (A-C) of HL such as HOMO–LUMO energy gap (ΔE), absolute electro negativities (χ), chemical potentials (μ), absolute hardness (η), absolute softness (σ), global softness (S) and additional electronic charge (ΔN_{max}) are calculated and given in Table 2 according to the following equations:^[7,15]

$$\Delta E = E_{LUMO} - E_{HOMO} \quad (2)$$

$$\chi = \frac{-(E_{HOMO} + E_{LUMO})}{2} \quad (3)$$

$$\eta = \frac{E_{LUMO} - E_{HOMO}}{2} \quad (4)$$

$$\sigma = \frac{1}{\eta} \quad (5)$$

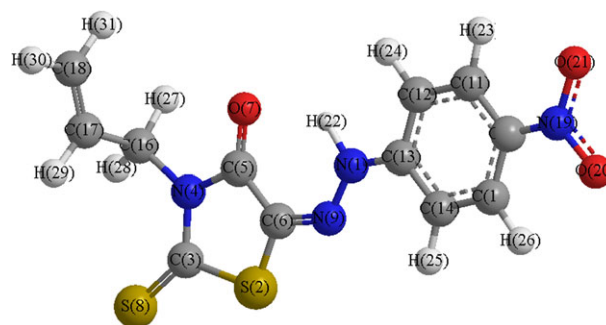


FIGURE 2 Optimized structure for keto hydrazone form (C) of HL

TABLE 2 The quantum chemical parameters for azo keto form (A), azo enol form (B) and keto hydrazone form (C) of HL

Form	E_{HOMO} (eV)	E_{LUMO} (eV)	ΔE (eV)	χ (eV)	η (eV)	σ (eV) ⁻¹	Pi (eV)	S (eV) ⁻¹	ΔN_{max}
(A)	-5.832	-3.303	2.529	4.568	1.265	0.791	-4.568	0.395	3.612
(B)	-4.571	-2.275	2.296	3.423	1.148	0.871	-3.423	0.436	2.982
(C)	-6.635	-4.400	2.235	5.518	1.118	0.895	-5.518	0.447	4.937

$$Pi = -\chi \quad (6)$$

$$S = \frac{1}{2\eta} \quad (7)$$

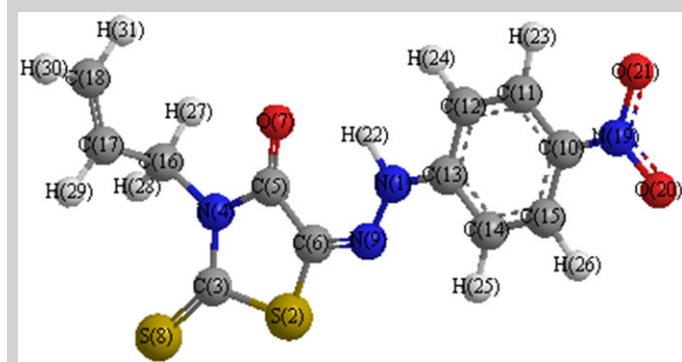
$$\Delta N_{\text{max}} = -\frac{Pi}{\eta} \quad (8)$$

The reactivity of the azo keto form (A), azo enol form (B) and keto hydrazone form (C) of HL can be predicted by considering the minimum HOMO–LUMO energy gap (ΔE). The value of ΔE for forms (A–C) of HL is 2.529, 2.296 and 2.235 eV, respectively. According to ΔE value, compound has minimum ΔE is the more stable, so keto hydrazone form (C) is more stable than the other forms (azo keto form (A), azo enol form (B)). The bond lengths and bond angles for keto hydrazone form (C) of HL are listed in Table S1. The computed net charges on active centers for the form (C) of HL are listed in Table 3, it is found that the most negative charge atoms in HL are N(1) and O(7) for keto hydrazone form (C) that makes it react stronger with the metal ion.

Molecular docking aims to achieve an optimized conformation for both the protein and drug with relative orientation between them such that the free energy of the overall system is minimized.^[3,20–22] In this context, we used molecular docking between the forms (A–C) of HL with the receptors of the prostate cancer (PDB code: 2Q7L Hormone) and the breast cancer (PDB code: 1JNX Gene regulation). The data showed a favorable arrangement between the forms (A–C) of HL and the receptors of the prostate cancer (PDB code: 2Q7L Hormone) and the breast cancer (PDB code: 1JNX Gene regulation) and the interaction curves are shown in Figures 3–5 and the calculated energy and some parameters with the receptors are listed in Table S2. The HB plot curves explain the interactions between forms (A–C) of HL and receptors (2Q7L and 1JNX) as shown in Figures S3–S5. The 2D plot curves of binding for forms (A–C) of HL with the receptors (2Q7L and 1JNX) are shown in Figures S6–S8, appear bending interaction sites of forms (A–C) of HL with proteins active sites of receptors. In general the more value with negative charge is the most stable interaction, where the free estimated free energy of binding, the estimated

TABLE 3 Net charges on active centers for keto hydrazone form (C) of HL

	Charges
N(1)	-0.458
S(2)	-0.282
N(4)	-0.420
O(7)	-0.570
S(8)	-0.380
N(9)	-0.442



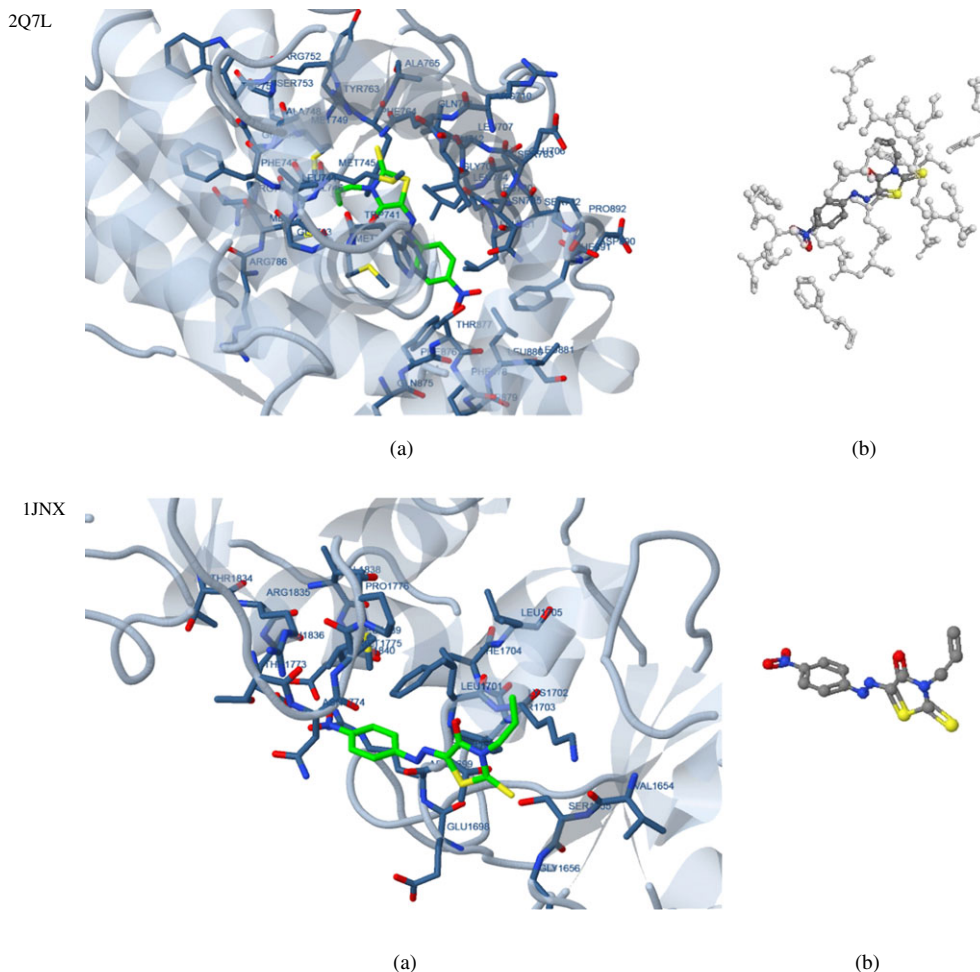


FIGURE 4 The monomer (form B) (green in (a) and gray in (b)) in interaction with receptors of 2Q7L and 1JNX

assigned to $\pi \rightarrow \pi^*$ (intra-ligand of aromatic system, C=C) and $n \rightarrow \pi^*$ transitions within the molecule (C=O), respectively.^[24] C=S group merge to form a single strong absorption band $\sim 30860 \text{ cm}^{-1}$. Most bands were slightly shifted in all the polymer complexes indicating coordination of the monomer to the metal. The band $\sim 22250 \text{ cm}^{-1}$ is characteristic for the ligand to metal charge transfer (LMCT) from the nitrogen atom to the transition metal center.

3.2.1 | Cobalt(II) polymer complex

The room temperature magnetic moment of the cobalt(II) polymer complex (5.05 B.M.) is characteristic of high-spin octahedral Co(II) polymer complex.^[6,15] IR spectrum of cobalt(II) polymer complex shows that the acetate group coordinate to Co(II) ion in a bidentate manner where the difference between the asymmetric and symmetric stretching vibrations of the acetate group is $\Delta\nu \leq 180 \text{ cm}^{-1}$.^[7] The electronic spectrum shows bands at 9620 cm^{-1} (${}^4T_{1g} \rightarrow {}^4T_{2g}(F)$) (ν_1),

15210 cm^{-1} (${}^4T_{1g} \rightarrow {}^4A_{2g}$) (ν_2) and 18700 cm^{-1} (${}^4T_{1g}(F) \rightarrow {}^4T_{1g}(P)$) (ν_3), suggesting that there is an octahedral geometry around Co(II) ion.^[6] Various ligand field parameters for the polymer complex were calculated and listed in Table 4. The nephelauxetic parameter (β) indicates appreciable covalent character in this polymer complex. The spectral parameters ν_2/ν_1 , $10Dq$, B and β were calculated and agreed well with the reported values for octahedral structure.

3.2.2 | Nickel(II) polymer complex

The Ni(II) polymer complex is paramagnetic and shows an effective magnetic moment of 2.80 B.M., which is within the range expected for two unpaired electron.^[25] Its electronic spectrum shows three bands at $\sim 10520 \text{ cm}^{-1}$ (${}^3A_{2g} \rightarrow {}^3T_{2g}(F)$) (ν_1), 19995 cm^{-1} (${}^3A_{2g} \rightarrow {}^3T_{1g}(F)$) (ν_2) and 24990 cm^{-1} (${}^3A_{2g} \rightarrow {}^3T_{1g}(P)$) (ν_3) transition, and this are suggestive of octahedral geometry around the nickel(II) ion.^[26] A small contribution because of spin-orbit coupling between the first

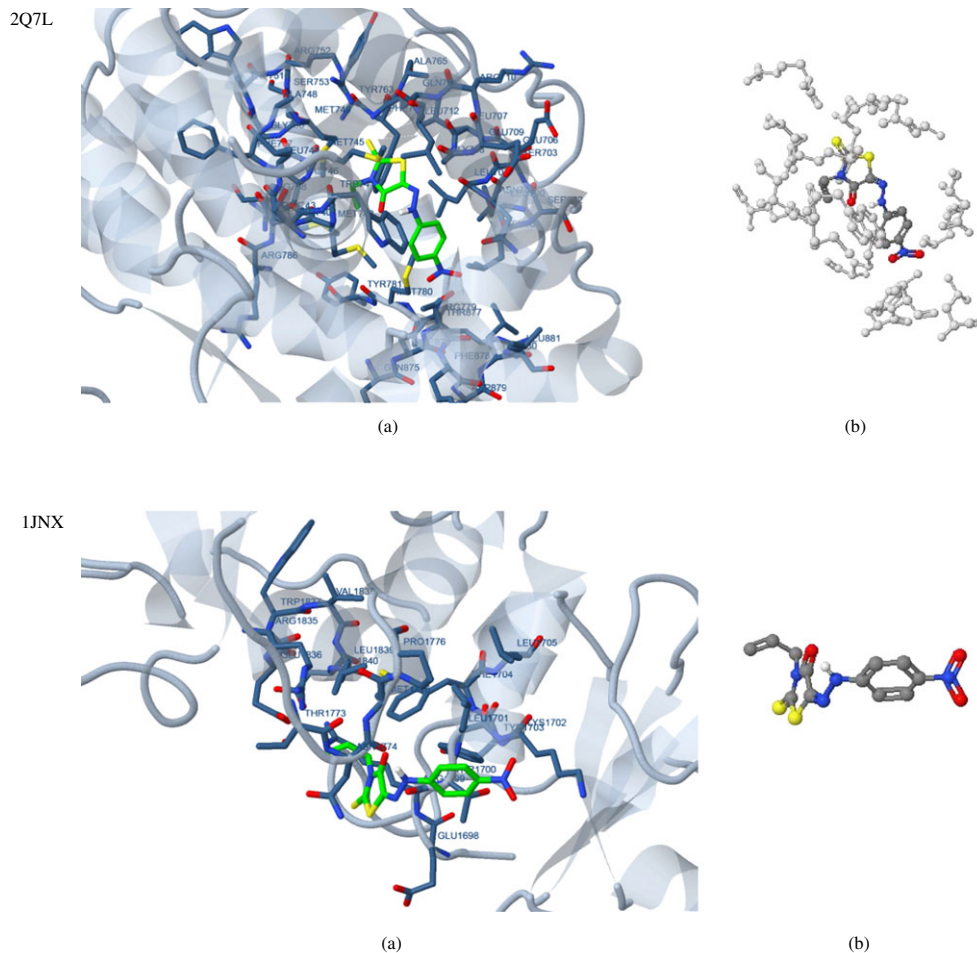


FIGURE 5 The monomer (form C) (green in (a) and gray in (b)) in interaction with receptors of 2Q7L and 1JNX

TABLE 4 Ligand field parameters of the polymer complexes

Complex ^a	ν_2/ν_1	$10Dq$ (cm ⁻¹)	B (cm ⁻¹)	β	β° (%)
(1)	1.58	8520	532	0.48	52
(2)	1.90	10520	895	0.86	14
(3)	1.18	18340	832	0.95	5
(4)	1.42	18580	425	0.46	54

^aNumbers as given in Table 1.

excited state ${}^3T_{2g}$ and the ground state ${}^3A_{2g}$ leads to a magnetic moment above the spin only value.^[27] The asymmetric and symmetric stretching vibrations of the acetate group appear at 1520 and 1384 cm⁻¹, respectively, for the nickel(II) acetate having the separation value $\Delta\nu = 136$ cm⁻¹ suggests the presence of bidentate chelating acetate group linked with Ni(II) ion center.^[12]

3.2.3 | Chromium(III) polymer complex

Chromium(III) polymer complex shows magnetic moment in the 3.89 B.M., which is in agreement with the presence

of three unpaired electrons. The presence of coordinated water molecule in the polymer complex is indicated by broad band at ~ 3500 cm⁻¹ and two weaker bands in ~ 780 and 705 cm⁻¹ due to $\nu(-OH)$ rocking and wagging mode of vibrations, respectively. Irrespective of the strength of the ligand field, three will be three unpaired electrons in binuclear Cr(III) polymer complex. The electronic spectrum of Cr(III) polymer complex exhibits three bands at ~ 18580 cm⁻¹ (${}^4A_{2g} \rightarrow {}^4T_{2g}$), 24910 cm⁻¹ (${}^4A_{2g} \rightarrow {}^4T_{1g}(F)$) and charge-transfer. From the electronic spectrum, it is concluded that Cr(III) polymer complex may have an octahedral geometry.^[28] Various ligand field parameters are calculated and given in Table 4. Dq value has been

evaluated by using Orgal energy level diagram. The nephelauxetic parameter (β) is obtained by using the relation: $\beta = B(\text{complex})/B(\text{free ion})$. The β value indicates that the polymer complex has appreciable covalent character.

3.2.4 | Manganese(II) polymer complex

The magnetic moment of the manganese(II) polymer complex at room temperature is 5.95 B.M., corresponding to five unpaired electrons. The electronic spectrum exhibits three bands at 22285 cm^{-1} (${}^6A_{1g} \rightarrow {}^4A_{1g}(\text{G})$, ${}^4E_g(\text{G})$) (ν_3), 21645 cm^{-1} (${}^6A_{1g} \rightarrow {}^4T_{2g}(\text{G})$) (ν_2) and 18340 cm^{-1} (${}^6A_{1g} \rightarrow {}^4T_{1g}(\text{G})$) (ν_1) transition, inside an octahedral configuration. Values of $10Dq$, Racah (B) and nephelauxetic parameters (18340 cm^{-1} , 832 cm^{-1} and 0.95) are calculated and indicate ionic character. The magnitude of $\Delta\nu = \nu_{\text{as}}(\text{COO}^-) - \nu_{\text{sym}}(\text{COO}^-) = 243\text{ cm}^{-1}$ suggest the coordination of acetate group in the monodentate fashion.^[16]

Various ligand parameters were calculated for the polymer complexes are listed in the Table 4. The value of β indicates the appreciable covalent character of metal sigma “ σ ” bond. The effect of covalence is to reduce the positive charge on the metal ion as a consequence of inductive effect to the ligand with reduced positive charge, the radial extension of the d-orbital increases.

By tracing the IR spectrum of uncomplexed azo, no νNH_2 of aniline stretching vibration is apparent.^[29] This supports the formation of azo monomer. The mode of bonding of the HL to the metal ions was elucidated by comparing the IR spectra of the polymer complexes with literature data for related systems.

The IR spectrum of monomer shows bands in the range of $3391\text{--}3255\text{ cm}^{-1}$ due to asymmetric and symmetric stretching vibrations of NH (hydrazone) group and intramolecular hydrogen bonding N-H...O systems (Figure 1). A strong band at $\sim 1604\text{ cm}^{-1}$ can guide to assume the presence of C=N- of hydrazone structure through resonating phenomena.^[6,30–32] In the IR spectrum, $\nu(\text{C}=\text{N}-\text{NH}$, hydrazone) band of monomer disappear in polymer complexes (**1**, **2** and **4**) but appear in polymer complex $[\text{Mn}(\text{HL})_2(\text{OCOCH}_3)_2]_n$ (**3**) (3382 cm^{-1} due to $-\text{C}=\text{N}-\text{NH}$), also adding more evidence for the hydrazone and deprotonation of the hydrazone proton (C=N-N-) prior to coordination of nitrogen to the metal ion and it is supported to a great extent by the appearance of a new peak due to $\nu(\text{M}-\text{N})$ stretching frequency. A strong band found at 1138 cm^{-1} is assigned to the $\nu(\text{N}-\text{N})$ band of the monomer. The positive shift of the frequency assigned to $\nu(\text{N}-\text{N})$ band in the spectra of polymer complexes is owing to the

coordination of nitrogen of hydrazone group. This has been confirmed by the bands in the $435\text{--}450\text{ cm}^{-1}$ range and it is assignable to the $\nu(\text{M}-\text{N})$ band.^[6] The presence of bands in the range of $1597\text{--}1594\text{ cm}^{-1}$ in polymer complexes due to asymmetric stretching vibration of the newly formed C=N- bond demonstrates the hydrazone structure of the monomer. The two intense carbonyl bands [$\nu(\text{C}=\text{O}\dots\text{H})$, $\nu(\text{C}=\text{O})$] of the monomer at 1702 cm^{-1} undergoes a negative shift of wavenumber in the polymer complexes indicating coordination *via* carbonyl oxygen. This has been confirmed by the bands in the $560\text{--}575\text{ cm}^{-1}$ range and it is assigned to the $\nu(\text{M}-\text{O})$.^[7] In Co(II) and Ni(II) polymer complexes (**1** and **2**), the bands of coordinated water observed at ~ 854 and $\sim 745\text{ cm}^{-1}$, are assigned to $\rho_r(\text{H}_2\text{O})$ and $\rho_w(\text{H}_2\text{O})$, respectively. Moreover, strong evidence for the presence or absence of water of crystallization and/or coordinated water supported by the thermogramme of all the polymer complexes. In Mn(II) polymer complex (**3**), the C=O and NH of hydrazone, stretching frequency bands observed at 1702 and $3391\text{--}3255\text{ cm}^{-1}$ for the free monomer and shifted to lower frequencies (~ 1676 and 3382 cm^{-1}) in polymer complex. This is due to the modification of hydrogen bonding interaction upon complex formation. The new additional bands observed with the difference $\Delta\nu = 243\text{ cm}^{-1}$ confirms the monodentate nature of the coordinated two acetate groups.^[16]

The ${}^1\text{H}$ NMR spectrum of HL supports the occurrence of the form depicted in Figure S10. The proton NMR spectra of the HL monomer and Cd(II) polymer complex (**5**) were recorded in DMSO- d_6 using tetramethylsilane (TMS) as the internal standard (Figure S10(a) and S11(a)). The protons of the aromatic ring resonate downfield in the range $7.48\text{--}8.25$ (4H) and $7.30\text{--}8.15$ ppm for HL and Cd(II) polymer complex (**5**), respectively. The broad signal at 11.40 ppm was assigned to intramolecular hydrogen bonded proton of NH (hydrazone) (Figure 1) which disappeared in the presence of D_2O (Figure S10(b)). The proton of NH (hydrazone) of HL and Cd(II) polymer complex (**5**) showed a signal at 11.64 ppm and 9.90 ppm, respectively. The shift of the proton of NH Cd(II) polymer complex (**5**) is due to the coordination of the nitrogen atom of NH (hydrazone) group with Cd(II) ion. The last two protons disappear in the presence of D_2O as shown in Figures S10(b) and S11(b). Absence of $-\text{CH}$ proton signal of rhodanine moiety and a new C=N-NH signal appear upon complexation, indicated the existence of the monomer in the keto hydrazone form. The ${}^1\text{H}$ NMR spectrum of HL showed the expected peaks and pattern of the vinyl group ($\text{CH}_2=\text{CH}$), i.e. 5.80 ppm for the vinyl CH proton and 4.60 ppm (*cis*) and 5.25 ppm (*trans*) for the vinyl CH_2 protons; these

peaks disappeared on polymerization. This indicates that the polymerization of HL occurs at the vinyl group.^[6] It is worth noting that the rest of the proton spectrum of HL remains almost without change. On the basis of all the above spectral data, an internally hydrogen bonded keto hydrazone structure has been proposed for the monomer (Figure 1).

3.3 | X-ray diffraction analysis

Single crystals of HL and its polymer complexes (**1–5**) could not be prepared to get the X-ray diffraction (XRD) and hence the powder diffraction data were obtained for structural characterization. Structure determination by X-ray powder diffraction data has gone through a recent

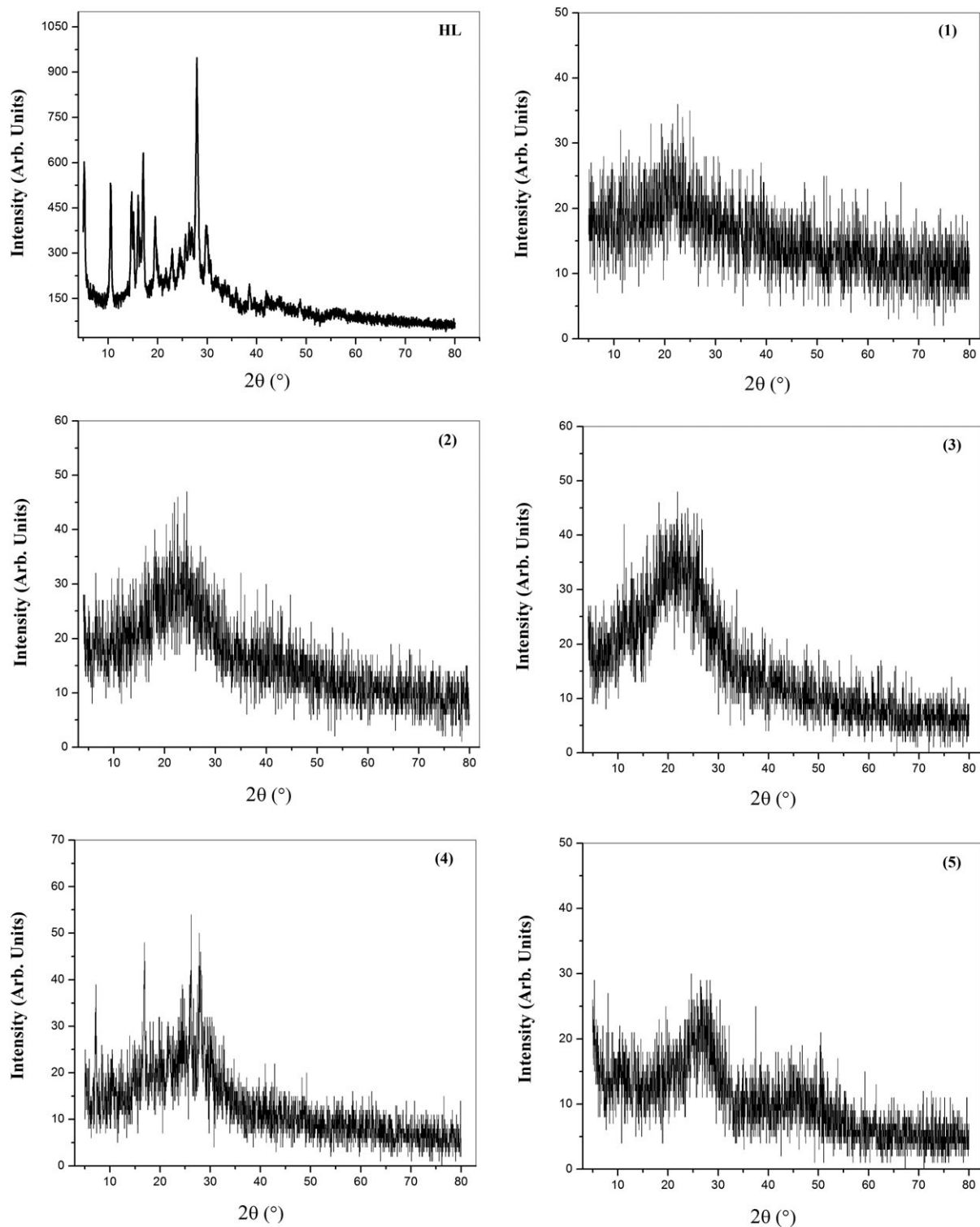


FIGURE 6 X-ray diffraction patterns of HL and its polymer complexes (**1–5**)

surge since it has become important to get to the structural information of materials, which do not yield good quality single crystals.

The X-ray diffraction analysis (XRD) patterns of HL and its polymer complexes (**1–5**) are shown in Figure 6. The XRD pattern of HL shows many diffraction peaks confirm the polycrystalline phase. The XRD patterns of polymer complexes (**1–5**) show in the range of $2\theta^\circ = 20 - 28^\circ$ a broad peak indicating a completely amorphous nature for these polymer complexes.^[6]

3.4 | Thermogravimetric analysis

The thermal decomposition of HL and its polymer complexes (**1–5**) was studied using the TG-technique.

The experiment was performed in temperature range from 30 to 800 °C at heating rate of 10 °C/min under dynamic nitrogen atmosphere. The thermogravimetric curves of polymer complexes (**1–5**) are shown in Figure 7. It was found that the thermal behaviors of the two polymer complexes (**1**) and (**2**) are similar. A three steps weight losing processes were involved in this experiment. The thermogravimetric analysis curves of HL and its polymer complexes (**1–5**) are shown in Figure 7 and loss of mass listed in Table 5.

The TG curve of the HL showed three steps of decomposition. The first step in the temperature range 125–313 °C attributed to loss of $C_6H_5NO_2$ (found 37.95%; calcd. 38.20%) and the second step in temperature range 313–764 °C attributed to loss of C_2HN_3OS

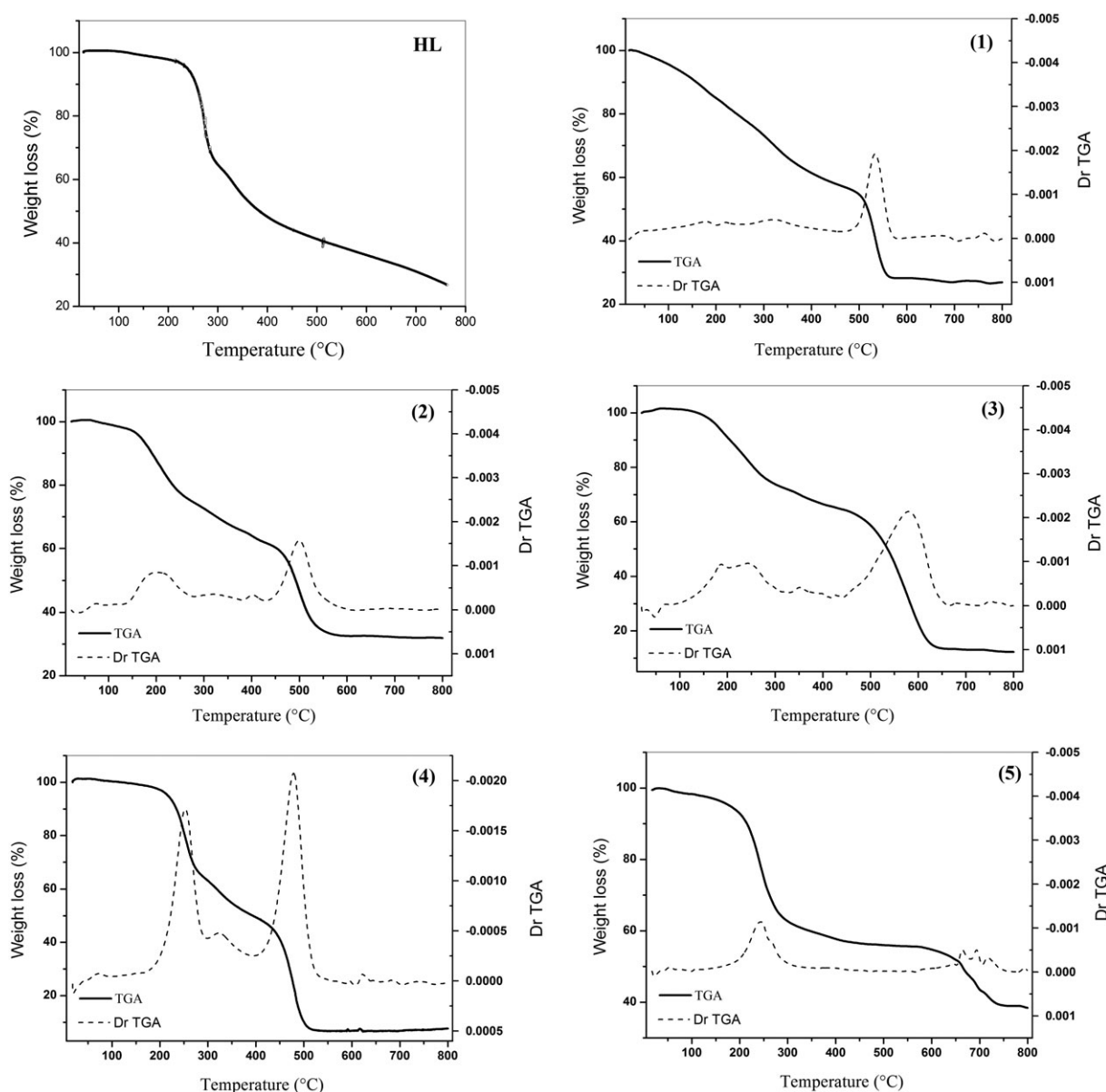


FIGURE 7 TGA curves of HL and its polymer complexes (**1–5**)

TABLE 5 Thermogravimetric analysis results of HL and its polymer complexes

Compound ^a	Temp. range (°C)	Found mass loss (calcd.) %	Assignment	Total mass loss Found (calcd.) %	Residue Found (calcd.) %
HL	125–313	37.95 (38.20)	Loss of C ₆ H ₅ NO ₂	100 (100)	-
	313–764	35.66 (35.71)	Loss of C ₂ HN ₃ OS		
	> 764	26.39 (26.09)	Loss of C ₄ H ₄ S		
(1)	50–134	7.53 (7.58)	Loss of two water molecules in inside of the coordination sphere.	74.05 (74.12)	CoO + 4 Carbon atoms 25.95 (25.88)
	134–390	30.66 (30.74)	Loss of acetate group and C ₃ H ₅ NS		
	390–800	35.86 (35.80)	Loss of C ₅ H ₄ N ₃ O ₂ S		
(2)	80–235	20.16 (20.01)	Loss of two water molecules in inside of the coordination sphere and acetate group.	71.78 (71.63)	NiO + 5 Carbon atoms 28.22 (28.37)
	235–438	18.40 (18.33)	Loss of C ₃ H ₅ NS		
	438–800	33.22 (33.29)	Loss of C ₄ H ₄ N ₃ O ₂ S		
(3)	140–278	24.33 (24.48)	Loss of two acetate groups and C ₆ H ₁₀	88.20 (88.38)	MnO + 2 Carbon atoms 11.80 (11.62)
	278–462	11.38 (11.26)	Loss of N ₂ O ₄		
	462–800	52.49 (52.64)	Loss of C ₁₆ H ₁₀ N ₆ OS ₄		
(4)	150–280	33.70 (34.18)	Loss of one water molecule in inside of the coordination sphere and C ₆ H ₁₀ N ₄ O ₄ Cl	89.32 (89.83)	½Cr ₂ O ₃ 10.68 (10.17)
	280–430	20.54 (20.33)	Loss of C ₂ S ₄		
	430–800	35.08 (35.32)	Loss of C ₁₆ H ₈ N ₄ O _{0.5}		
(5)	50–280	33.13 (34.21)	Loss of two acetate groups and C ₃ H ₅ NO	67.58 (68.06)	CdO + 4 Carbon atoms 32.42 (31.94)
	280–595	12.79 (12.67)	Loss of C ₂ NS		
	595–800	21.66 (21.18)	Loss of C ₃ H ₅ N ₂ OS		

^aNumbers as given in Table 1.

(found 35.66%; calcd. 35.71%). Third step represented the loss of C₄H₄S at >764 °C (mass loss: found 26.39%, calcd. 26.09%).

For Co(II) polymer complex **(1)**, according to Figure 7, the first weight loss of 7.53% corresponding to the loss of two water molecules in inside of the coordination sphere (calcd. 7.58%) occurred in temperature range 50–134 °C. The second weight loss of 30.66% corresponding to the loss of acetate group and C₃H₅NS (calcd. 30.74%) occurred in the range of 134–390 °C. The third weight loss of 35.86% corresponding to the loss of C₅H₄N₃O₂S (calcd. 35.80%) occurred in the range of 390–800 °C. CoO and four carbon atoms is a residue with mass percent of 25.95% (calcd. 25.88%).

The thermogram of Ni(II) polymer complex **(2)** showed three decomposition steps. The first decomposition step within the temperature range 80–235 °C corresponded to the loss of two water molecules in inside of the coordination sphere and acetate group with a mass loss of 20.16% (calcd. 20.01%) and the second decomposition step at 235–438 °C which related to loss of C₃H₅NS (found 18.40%; calcd. 18.33%). The third step in the temperature range of 438–800 °C corresponded to the loss of C₄H₄N₃O₂S with a mass loss of 33.22% (calcd. 33.29%) and left NiO and five carbon atoms as a residue with mass percent of 28.22% (calcd. 28.37%).

The Mn(II) polymer complex **(3)** began decomposing at 140 °C in three decomposition steps. The first step of decomposition found within the temperature range of 140–278 °C corresponded to loss of two acetate groups and C₆H₁₀. It represented weight loss of 24.33%, which is in good agreement with the calculated value of 24.48%. The second step of decomposition found within the temperature range of 278–462 °C which was assigned to loss of N₂O₄. It represented a weight loss of 11.38% which is in good agreement with the calculated value of 11.26%. The third step of decomposition found within the temperature range of 462–800 °C which was assigned to loss of C₁₆H₁₀N₆OS₄. It represented a weight loss of 52.49% which is in good agreement with the calculated value of 52.64%. The decomposition of this polymer complex ended with leaving MnO and two carbon atoms residue with mass percent of 11.80% (calcd. 11.62%).

Cr(III) polymer complex **(4)** was thermally stable up to 150 °C. Decomposition of the polymer complex began at 150 °C to 800 °C. The thermal decomposition of this polymer occurred completely in three steps. The first decomposition step within the temperature range 150–280 °C corresponded to the loss of coordinated water molecule and C₆H₁₀N₄O₄Cl with a mass loss of 33.70% (calcd. 34.18%) and the second decomposition step at 280–430 °C

which related to loss of C_2S_4 (found 20.54%; calcd. 20.33%). The third decomposition step within the temperature range of 430–800 °C corresponded to the loss of $C_{16}H_8N_4O_{0.5}$ with a mass loss of 35.08% (calcd. 35.32%) and leaved $\frac{1}{2}Cr_2O_3$ as a residue with mass percent of 10.68% (calcd. 10.17%).

The thermal analysis curve of Cd(II) polymer complex (**5**) indicated that decomposition took place in three decomposition steps. The first and second steps of decomposition within the temperature range of 50–280 °C and 280–595 °C, have weight loss about 33.13% (calcd. 34.21%) and 12.79% (calcd. 12.67%), and was attributed to the loss of two acetate groups, C_3H_5NO and C_2NS , respectively. Third step represented the loss of $C_3H_5N_2OS$ at 595–800 °C (mass loss: found 21.66%, calcd. 21.18%) to give finally CdO and four carbon atoms as a residue with mass percent of 32.42% (calcd. 31.94%).

3.5 | Kinetic studies

The thermodynamics parameters of HL and its polymer complexes (**1–5**) as the thermal activation energy of

decomposition (E_a), enthalpy (ΔH^*), Gibbs free energy change of the decomposition (ΔG^*) and entropy (ΔS^*) are calculated by Coast-Redfern and Horowitz-Metzger methods.^[33,34] The enthalpy (ΔH^*) and Gibbs free energy of decomposition (ΔG^*) were calculated by $\Delta H^* = E_a - RT$ and $\Delta G^* = \Delta H^* - T\Delta S^*$, respectively. The thermodynamics parameters obtained with the Coast-Redfern and Horowitz-Metzger methods for of HL and its polymer complexes (**1–5**) are listed in Table 6 (Figures 8 and 9). The thermodynamics parameters data obtained from the two methods of Coast-Redfern and Horowitz-Metzger methods are comparable and can be considered in good agreement with each other.^[35,36] The data obtained are summarized in the following:

1. The values of ΔG^* for HL and its polymer complexes are positive values and confirmed the process is non-spontaneous.
2. The values of ΔS^* for HL and its polymer complexes are negative values indicate the reaction is slow or more ordered activated polymer complex than the reactants.^[12,36]

TABLE 6 Thermodynamic data of the thermal decomposition of HL and its polymer complexes

Compound ^a	Decomposition temperature (°C)	Method	Thermodynamic parameters				Correlation coefficient
			E_a (kJ mol ⁻¹)	ΔS^* (J mol ⁻¹ K ⁻¹)	ΔH^* (kJ mol ⁻¹)	ΔG^* (kJ mol ⁻¹)	
HL	185-307	CR	119	-73.2	115	153	0.98975
		HM	120	-57.1	116	146	0.99572
	307-490	CR	52.2	-224	46.7	197	0.99364
		HM	63.0	-207	57.4	196	0.99223
(1)	50-395	CR	21.3	-267	17.2	149	0.98744
		HM	24.7	-251	20.6	145	0.99345
	395-565	CR	106	-181	99.5	236	0.99623
		HM	110	-153	104	219	0.99254
(2)	95-402	CR	30.7	-248	26.3	156	0.99313
		HM	38.2	-225	33.9	151	0.99339
	402-545	CR	153	-108	147	227	0.99004
		HM	145	-102	139	215	0.99664
(3)	140-278	CR	52.5	-190	48.5	140	0.98724
		HM	60.2	-168	56.2	137	0.98889
	278-462	CR	46.8	-231	41.5	190	0.98918
		HM	56.8	-212	51.4	188	0.99095
(4)	155-280	CR	83.8	-117	79.7	137	0.99256
		HM	93.0	-100	88.9	138	0.99850
	280-430	CR	59.7	-206	54.4	184	0.99093
		HM	68.0	-190	62.8	182	0.99085
(5)	130-280	CR	65.1	-148	61.1	132	0.99329
		HM	74.4	-135	70.4	135	0.9965
	280-595	CR	26.0	-281	20.1	220	0.98702
		HM	29.2	-267	23.3	213	0.99086

^aNumbers as given in Table 1.

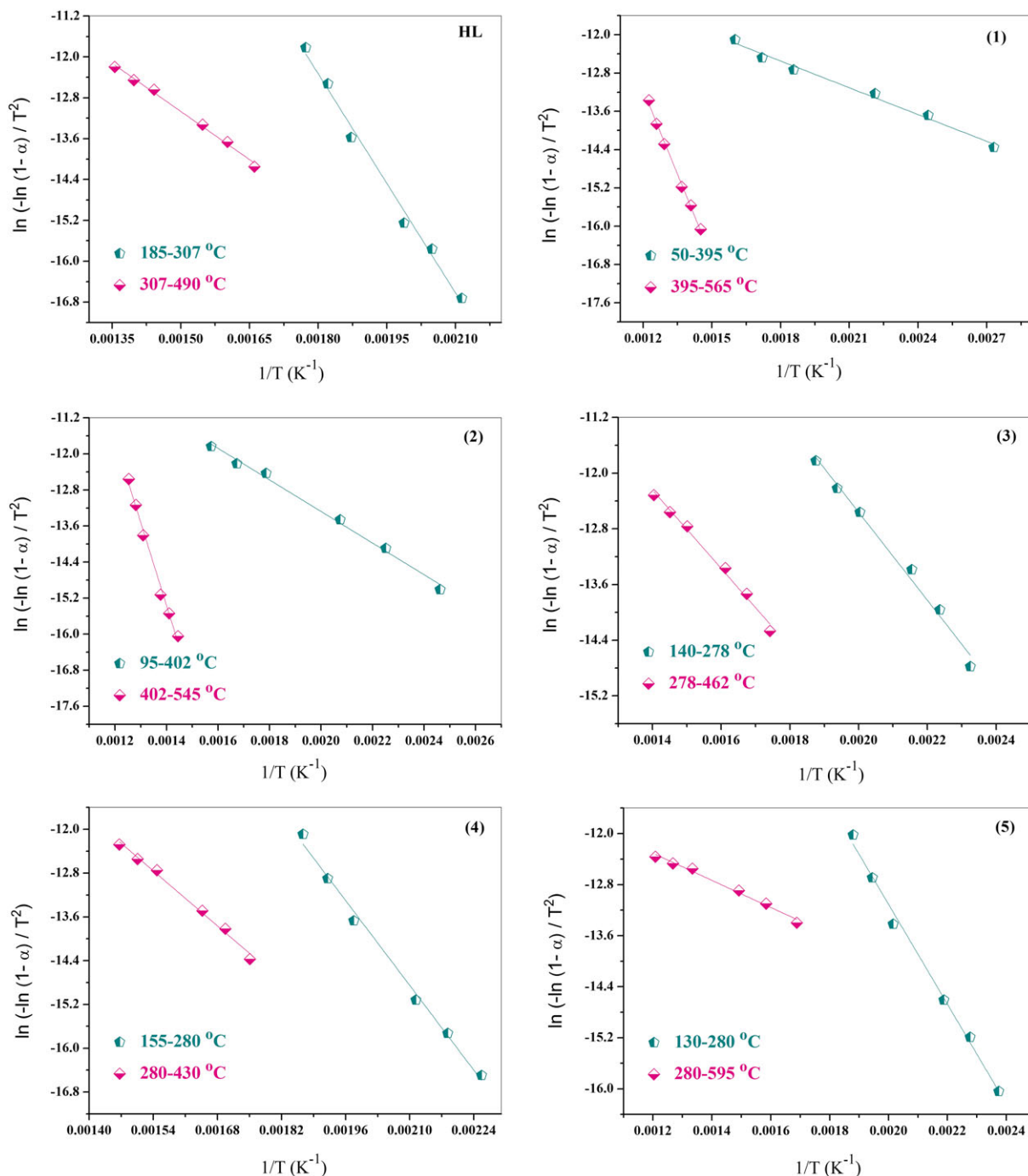


FIGURE 8 Coats-Redfern (CR) of HL and its polymer complexes (1-5)

- The value of the thermal activation energy of decomposition (E_a) for the HL is the highest than the polymer complexes.
- The E_a value of Ni(II) polymer complex (2) is higher than the E_a value of Co(II) polymer complex (1).^[15]

3.6 | DNA binding study

DNA is one of the most important biomacromolecules in life processes because it carries inheritance

information and instructs the biological synthesis.^[7,35,37] The intercalation of HL and its polymer complexes with Calf thymus DNA (CT-DNA) is carried out using absorption spectroscopy to determine the intrinsic binding constant (K_b) to CT-DNA. In presence of DNA, the absorption bands of the HL and its polymer complexes (1-5) exhibited hypochromism and red shift of about 1-4 nm at about 433, 414, 420, 345, 431 and 430 nm for HL and its polymer complexes (1-5), respectively, (Figure S12). It was found that the absorption bands of the HL and its polymer complexes decrease with

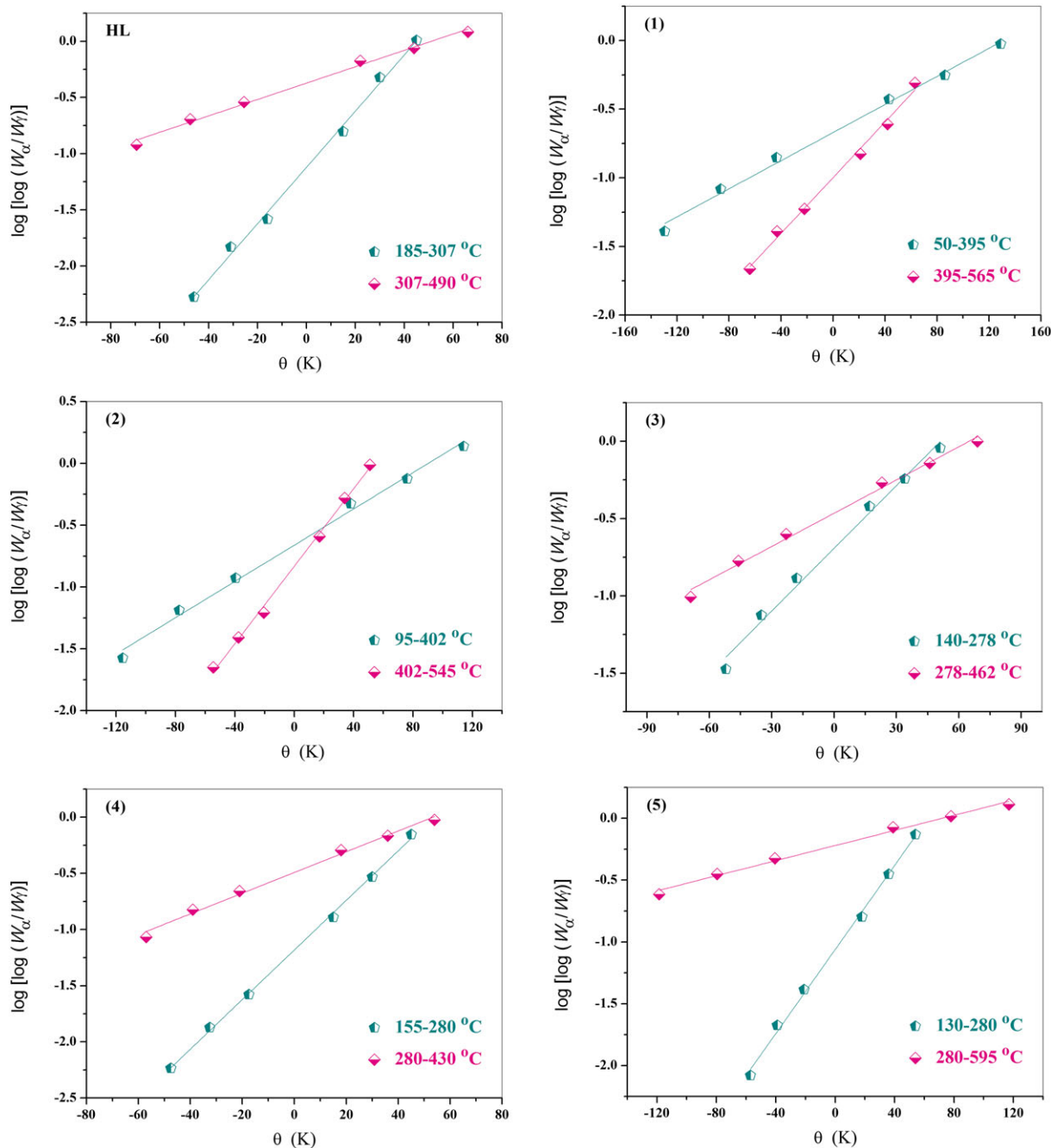


FIGURE 9 Horowitz-Metzger (HM) of HL and its polymer complexes (1–5)

increasing concentration of CT-DNA.^[12] In plots of $[\text{DNA}]/(\epsilon_a - \epsilon_f)$ versus $[\text{DNA}]$ (Figure S12) were determined intrinsic binding constants (K_b). The value of intrinsic binding constant (K_b) of HL with CT-DNA was determined and it was found that the complexation lead to increases of the K_b value than HL free.

The values of intrinsic binding constant (K_b) for HL and its polymer complexes (1–5) are calculated and found to be 1.80×10^4 , 8.16×10^4 , 9.89×10^4 , 3.37×10^4 , 2.62×10^5 and 1.57×10^5 , respectively. From the values of intrinsic binding constant (K_b) show

Ni(II) polymer complex (2) has high value of K_b with compared to Co(II) polymer complex (1) may be due to the lower ionic radius of Ni(II) with compared to Co(II).^[15] Also it was found that the Cr(III) polymer complex (4) is the highest value of K_b than HL and polymer complexes (1–3 and 5), this indicated that the Cr(III) polymer complex (4) is highly binding with CT-DNA. The polymer complexes revealed higher efficient binding to DNA than HL monomer and these varieties in K_b values of polymer complexes are mainly due to the effect of the type of metal and the coordinated sphere groups (acetate or chloride).

3.7 | Antimicrobial activities study

Antifungal and antibacterial activities of HL and polymer complexes (**1–5**) were examined and the data were recorded in Tables 7 and 8. HL has antibacterial activity against *Bacillus subtilis* and *Staphylococcus aureus* and the inhibition zone was 17 and 15 mm, respectively, and has antibacterial activity against *Escherichia coli* and *Salmonella typhimurium* and the inhibition zone was 18 and 17 mm, respectively.

Co(II) polymer complex (**1**) and Mn(II) polymer complex (**3**) have no antibacterial activity against *Bacillus subtilis*, *Staphylococcus aureus*, *Escherichia coli* and *Salmonella typhimurium*. Ni(II) polymer complex (**2**) has no antibacterial activity against *Bacillus subtilis* and *Staphylococcus aureus* but has antibacterial activity against *Escherichia coli* and *Salmonella typhimurium* and the inhibition zone was 12 and 11 mm, respectively. Cr(III) polymer complex (**4**) has antibacterial activity against *Bacillus subtilis* and *Staphylococcus aureus* and the inhibition zone was 20 and 21 mm, respectively, as well as has antibacterial activity against *Escherichia coli* and *Salmonella typhimurium* and the inhibition zone was 15 and 21 mm, respectively. It was found that Cr(III) polymer complex (**4**) is more antibacterial activity than the Gentamycin (standard of antibacterial drug) against *Salmonella typhimurium*. The activity of the Cr(III) polymer complex (**4**) may be because of there are one chloride ion, type of the metal and 1:2 molar ratio.^[38] Cd(II) polymer complex (**5**) has antibacterial activity against *Bacillus subtilis* and *Staphylococcus aureus* and the inhibition zone was 15 and 16 mm, respectively, as well as has antibacterial activity against *Escherichia coli* and *Salmonella typhimurium* and the inhibition zone was 14 and 15 mm, respectively.

From these results it was found that the Cr(III) polymer complex (**4**) is more antibacterial activity

than HL and polymer complexes (**1–3** and **5**) against *Bacillus subtilis*, *Staphylococcus aureus* and *Salmonella typhimurium*. There are six factors that govern the biological activity of the metal complexes: (i) the nature of the donor atoms, (ii) the chelate effect of the monomer, (iii) the nature of the metal ion, (iv) the total charge on the complex ion, (v) the geometrical structure of the complex and (vi) the nature of the counter ions that neutralize the complex.^[35,38]

The results of the antifungal activity of the HL and polymer complexes (**1–5**) are listed in Table 8. HL and polymer complexes (**1–3**) have no antifungal activity against *Aspergillus fumigatus* and *Candida albicans* but Cr(III) and Cd(II) polymer complexes (**4** and **5**) have effects against *Aspergillus fumigatus* and *Candida albicans*.

From a comparative study of the growth inhibition zone values of antifungal activity for HL and polymer complexes (**1–5**), it is found that the Cr(III) and Cd(II) polymer complexes (**4** and **5**) have higher activity than the HL against

TABLE 8 Antifungal activity data of HL and its metal polymer complexes (**1–5**). The results are recorded as the diameter of inhibition zone (mm)

Compound ^a	<i>Aspergillus fumigatus</i>	<i>Candida albicans</i>
HL	-ve	-ve
(1)	-ve	-ve
(2)	-ve	-ve
(3)	-ve	-ve
(4)	20	10
(5)	22	11
Ketoconazole (Standard of antifungal drug)	17	20

^aNumbers given in Table 1.

TABLE 7 Antibacterial activity data of HL and its metal polymer complexes (**1–5**). The results are recorded as the diameter of inhibition zone (mm)

Compound ^a	Gram positive bacteria		Gram negative bacteria	
	<i>Bacillus subtilis</i>	<i>Staphylococcus aureus</i>	<i>Escherichia coli</i>	<i>Salmonella typhimurium</i>
HL	17	15	18	17
(1)	-ve	-ve	-ve	-ve
(2)	-ve	-ve	12	11
(3)	-ve	-ve	-ve	-ve
(4)	20	21	15	21
(5)	15	16	14	15
Gentamycin (Standard of antibacterial drug)	26	24	30	17

^aNumbers given in Table 1.

Aspergillus fumigatus and *Candida albicans* as shown in Table 8. Our results are similar to Habib *et al.*^[39] who studied the antimicrobial activities of some rhodanine derivatives and they revealed that the most pronounced activity was the antifungal activity against *Aspergillus niger*.

4 | CONCLUSION

3-Allyl-5-[(4-nitrophenylazo)]-2-thioxothiazolidine-4-one (HL) and its Co(II), Ni(II), Mn(II), Cr(III) and Cd(II) polymer complexes were prepared and characterized by elemental analysis, IR spectra and thermal analysis. The X-ray diffraction analysis (XRD) pattern of HL shows many diffraction peaks confirm the polycrystalline phase. The values of intrinsic binding constant (K_b) for HL and its polymer complexes (**1–5**) are calculated and it was found that the Cr(III) polymer complex (**4**) is the highest value of K_b than HL and polymer complexes (**1–3** and **5**), this indicated that the Cr(III) polymer complex (**4**) is highly binding with CT-DNA. The value of the thermal activation energy of decomposition (E_a) for the HL is the highest than the polymer complexes. Cr(III) polymer complex (**4**) has more antibacterial activity than HL and polymer complexes (**1–3** and **5**) against *Bacillus subtilis*, *Staphylococcus aureus* and *Salmonella typhimurium*. As well as Cr(III) and Cd(II) polymer complexes (**4** and **5**) have effects against *Aspergillus fumigatus* and *Candida albicans*.

ORCID

M.A. Diab  <http://orcid.org/0000-0002-9042-1356>

A.Z. El-Sonbati  <http://orcid.org/0000-0001-7059-966X>

Sh.M. Morgan  <http://orcid.org/0000-0002-8921-4894>

REFERENCES

- [1] R. Rajgopal, S. Seshadri, *Dyes Pigm.* **1999**, *13*, 93.
- [2] M. I. Abou-Dobara, A. Z. El-Sonbati, Sh. M. Morgan, *World J. Microbiol. Biotechnol.* **2013**, *29*, 119.
- [3] Sh. M. Morgan, M. A. Diab, A. Z. El-Sonbati, *Appl. Organometal. Chem.* **2018**, *32*, e4281. <https://doi.org/10.1002/aoc.4281>
- [4] W. Moreda, A. R. Forrester, *Tetrahedron* **1997**, *53*, 295.
- [5] T. Ayesha, A. Lycka, S. Lunak, O. Machalicky, M. Elselik, R. Hirdina, *Dyes Pigm.* **2013**, *98*, 547.
- [6] Sh. M. Morgan, A. Z. El-Sonbati, M. A. El-Mogazy, *Appl. Organometal. Chem.* **2018**, *32*, e4264. <https://doi.org/10.1002/aoc.4264>
- [7] Sh. M. Morgan, M. A. Diab, A. Z. El-Sonbati, *Appl. Organometal. Chem.* **2018**, *32*, e4305. <https://doi.org/10.1002/aoc.4305>
- [8] N. A. El-Ghamaz, A. Z. El-Sonbati, Sh. M. Morgan, *J. Mol. Struct.* **2012**, *1027*, 92.
- [9] Sh. M. Morgan, N. A. El-Ghamaz, M. A. Diab, *J. Mol. Struct.* **2018**, *1160*, 227.
- [10] N. A. El-Ghamaz, M. A. Diab, A. Z. El-Sonbati, Sh. M. Morgan, O. L. Salem, *Chem. Pap.* **2017**, *71*, 2417.
- [11] (a) N. A. El-Ghamaz, A. Z. El-Sonbati, M. A. Diab, A. A. El-Bindary, Sh. M. Morgan, *Mater. Res. Bull.* **2015**, *65*, 293. (b) N. A. El-Ghamaz, A. Z. El-Sonbati, M. A. Diab, A. A. El-Bindary, G. G. Mohamed, Sh. M. Morgan, *Spectrochim. Acta A* **2015**, *147*, 200. (c) N. A. El-Ghamaz, A. Z. El-Sonbati, M. A. Diab, A. A. El-Bindary, M. K. Awad, Sh. M. Morgan, *Mater. Sci. Semicond. Proc.* **2014**, *19*, 150.
- [12] A. Z. El-Sonbati, M. A. Diab, Sh. M. Morgan, *J. Mol. Liq.* **2017**, *225*, 195.
- [13] M. A. Diab, A. Z. El-Sonbati, A. A. El-Bindary, M. Z. Balboula, *J. Mol. Struct.* **2013**, *1040*, 171.
- [14] (a) A. Z. El-Sonbati, M. A. Diab, *Polym. Deg. Stab.* **1988**, *22*, 295. (b) M. A. Diab, A. Z. El-Sonbati, A. A. El-Sanabari, *Polym. Deg. Stab.* **1988**, *23*, 83. (c) M. A. Diab, A. Z. El-Sonbati, A. A. El-Sanabari, *Polym. Deg. Stab.* **1989**, *24*, 51.
- [15] Sh. M. Morgan, A. Z. El-Sonbati, H. R. Eissa, *J. Mol. Liq.* **2017**, *240*, 752.
- [16] A. Z. El-Sonbati, M. A. Diab, Sh. M. Morgan, M. Z. Balboula, *Appl. Organometal. Chem.* **2018**, *32*, e4059. <https://doi.org/10.1002/aoc.4059>
- [17] National Committee for Clinical Laboratory Standards. Method for Antifungal Disc Diffusion Susceptibility Testing of Yeast: Proposed Guideline M44-P. Wayne, PA, USA, **2003**.
- [18] J. Bassett, R. C. Denney, G. H. Jeffery, J. Mendham, *Vogel's Textbook of Quantitative Inorganic Analysis*, London Group Limited, London **1978**.
- [19] P. W. Selwood, *Magnetic Chemistry*, Interscience Pub. Inc., New York **1956**.
- [20] H. M. Refaat, H. A. El-Badway, Sh. M. Morgan, *J. Mol. Liq.* **2016**, *220*, 802.
- [21] G. G. Mohamed, A. A. El-Sherif, M. A. Saad, S. E. A. El-Sawy, Sh. M. Morgan, *J. Mol. Liq.* **2016**, *223*, 1311.
- [22] A. A. El-Bindary, G. G. Mohamed, A. Z. El-Sonbati, M. A. Diab, W. M. I. Hassan, Sh. M. Morgan, A. K. Elkholy, *J. Mol. Liq.* **2016**, *218*, 138.
- [23] A. Z. El-Sonbati, M. A. Diab, Sh. M. Morgan, H. A. Seyam, *J. Mole. Struct.* **2018**, *1154*, 354.
- [24] M. C. Jain, A. K. Shrivastava, P. C. Jain, *Inorg. Chim. Acta* **1977**, *23*, 199.
- [25] R. S. Drago, *Physical Methods in Inorganic Chemistry*, Vol. 395, East West Press, New Delhi **1971** 328.
- [26] A. B. P. Lever, *Inorganic Electronic Spectroscopy*, Elsevier, Amsterdam **1984**.
- [27] A. B. P. Lever, *Crystall Field Spectra Inorganic Electronic Spectroscopy*, First ed., Elsevier, Amsterdam **1968** 249.
- [28] S. Chandra, L. K. Gupta, *Orient. J. Chem.* **2003**, *19*, 570.

- [29] A. Z. El-Sonbati, G. G. Mohamed, A. A. El-Bindary, W. M. I. Hassan, M. A. Diab, Sh. M. Morgan, A. K. Elkholy, *J. Mol. Liq.* **2015**, 212, 487.
- [30] A. Z. El-Sonbati, A. A. M. Belal, M. S. El-Gharib, Sh. M. Morgan, *Spectrochim. Acta A* **2012**, 95, 627.
- [31] A. Z. El-Sonbati, M. A. Diab, A. A. M. Belal, Sh. M. Morgan, *Spectrochim. Acta A* **2012**, 99, 353.
- [32] A. Z. El-Sonbati, M. A. Diab, A. A. El-Bindary, A. M. Eldesoky, Sh. M. Morgan, *Spectrochim. Acta A* **2015**, 135, 774.
- [33] A. W. Coats, J. P. Redfern, *Nature* **1964**, 201, 68.
- [34] H. H. Horowitz, G. Metzger, *Anal. Chem.* **1963**, 35, 1464.
- [35] A. Z. El-Sonbati, M. A. Diab, Sh. M. Morgan, A. M. Eldesoky, M. Z. Balboula, *Appl. Organometal. Chem.* **2018**, 32, e4207. <https://doi.org/10.1002/aoc.4207>
- [36] A. Z. El-Sonbati, M. A. Diab, A. A. El-Bindary, G. G. Mohamed, Sh. M. Morgan, M. I. Abou-Dobara, S. G. Nozha, *J. Mol. Liq.* **2016**, 215, 423.
- [37] S. Rajalakshmi, T. Weyhermuller, A. J. Freddy, H. R. Vasanthi, B. U. Nair, *Eur. J. Med. Chem.* **2011**, 46, 608.
- [38] A. Z. El-Sonbati, A. A. El-Bindary, G. G. Mohamed, Sh. M. Morgan, W. M. I. Hassan, A. K. Elkholy, *J. Mol. Liq.* **2016**, 218, 16.
- [39] N. S. Habib, Sh. M. Rida, E. A. M. Badawey, H. T. Y. Fahmy, H. A. Ghozlan, *Eur. J. Med. Chem.* **1997**, 32, 759.

SUPPORTING INFORMATION

Additional Supporting Information may be found online in the supporting information tab for this article.

How to cite this article: Diab MA, El-Sonbati AZ, Morgan ShM, El-Mogazy MA. Polymer complexes. LXXI. Spectroscopic studies, thermal properties, DNA binding and antimicrobial activity of polymer complexes. *Appl Organometal Chem.* 2018;e4378. <https://doi.org/10.1002/aoc.4378>